Published in final edited form as:

Comp Biochem Physiol A Mol Integr Physiol. 2024 October ; 296: 111685. doi:10.1016/j.cbpa.2024.111685.

Function and regulation of the insect NaCCC2 sodium transport proteins

Ryan S. Yarcusko[1,$], **Maria Hemmi Song**[1,$], **Grace C. Neuger**[1,$], **Michael F. Romero**[2], **Peter M. Piermarini**[3], **Christopher M. Gillen**[#,1]

[1]Department of Biology, Kenyon College, Gambier, OH 43050, USA

[2]Physiology and Biomedical Engineering, Mayo Clinic College of Medicine and Science, Rochester, MN 55902, USA

[3]Department of Entomology, The Ohio State University, Ohio Agricultural Research and Development Center, Wooster, OH 44691, USA

Abstract

NaCCC2 transport proteins, including those from *Drosophila melanogaster* (Ncc83) and *Aedes aegypti* (aeCCC2), are an insect-specific clade with sequence similarity to Na^+-K^+−$2Cl^−$ cotransporters. Whereas the Na^+-K^+−$2Cl^−$ cotransporters and other cation-chloride cotransporters are electroneutral, recent work indicates that Ncc83 and aeCCC2 carry charge across membranes. Here, we further characterize the regulation and transport properties of Ncc83 and aeCCC2 expressed in *Xenopus* oocytes. In cation uptake experiments, Li^+ was used as a tracer for Na^+ and Rb^+ was used as a tracer for K^+. Li^+ uptake of oocytes expressing either aeCCC2 or Ncc83 was greater than uptake in water-injected controls, activated by hypotonic swelling, and not inhibited by ouabain or ethyl cinnamate. Rb^+ uptake of oocytes expressing either aeCCC2 or Ncc83 was not different than water injected controls. In oocytes expressing either aeCCC2 or Ncc83, Li^+ uptake plateaued with increasing Li^+ concentrations, with apparent K_m values in the range of 10 to 20 mM. Following exposure to ouabain, intracellular [Na^+] was greater in oocytes expressing aeCCC2 than in controls. Elevating intracellular cAMP (via 8-bromo-cAMP) in Ncc83 oocytes significantly stimulated both Li^+ uptake and membrane conductances. Elevating intracellular cAMP in aeCCC2 oocytes did not affect Li^+ uptake, but stimulated membrane conductances. Overall, these results confirm that the NaCCC2s resemble other cation-chloride cotransporters in their regulation and some transport properties. However, unlike other cation-chloride cotransporters, they carry charge across membranes.

Keywords

cation-chloride cotransporter; membrane potential; *Aedes aegypti* ; *Drosophila melanogaster* ; epithelial transport

Corresponding author: Christopher M. Gillen, Department of Biology, Kenyon College, Gambier, OH 43050, gillenc@kenyon.edu.
$These authors contributed equally to this work.

Introduction

The cation-chloride cotransporter family (CCC, SLC12a) of membrane transport proteins has diversified during evolutionary history through gene duplication and loss, as well as by neo- and sub-functionalization (Hartmann et al., 2014). NaCCC2s (Na^+-dependent cation-chloride cotransporters) are insect CCCs that are closely related to the well-characterized NKCCs (Na^+-K^+−$2Cl^-$ cotransporters) (Piermarini et al., 2017). Vertebrate and insect Na^+-K^+−$2Cl^-$ cotransporters have electroneutral stoichiometry; they carry positively and negatively charged ions across cell membranes in equal proportion (Delpire and Guo, 2020; Payne, 2012). In contrast, recent studies suggest that NaCCC2s carry net charge across cell membranes (Duong et al., 2022; Kalsi et al., 2019). Oocytes expressing *Aedes aegypti* aeCCC2 or *Drosophila melanogaster* Ncc83 (also called NKCC) have greater Na^+-dependent conductances in voltage-clamp experiments. Moreover, compared to H_2O-injected controls, oocytes expressing aeCCC2 are characterized by increased Li^+ (a tracer for Na^+) uptake, that is independent of external Cl^- (Kalsi et al., 2019).

Sequence comparisons between the NaCCC2s and Na^+-K^+−$2Cl^-$ cotransporters suggest structural explanations for functional differences, especially when interpreted in the context of recent cryo-EM structures of vertebrate Na^+-K^+−$2Cl^-$ cotransporters (Chew et al., 2019; Liu et al., 2019; Yang et al., 2020). Notably, amino acids at key residues in the K^+ and Cl^- binding pockets of vertebrate Na^+-K^+−$2Cl^-$ cotransporters differ between the NaCCC2s (aeCCC2 and Ncc83) and the Na^+-K^+−$2Cl^-$ homologs in mosquitoes (aeNKCC1) and *Drosophila* (Ncc69) (Duong et al., 2022). For example, substitutions at locations in transmembrane domains 1 and 6 involved in Cl^- binding are consistent with the ability of aeCCC2 to function in the absence of external Cl^- (Kalsi et al., 2019). In contrast, binding and phosphoacceptor sites for SPAK kinases, which activate Na^+-K^+−$2Cl^-$ cotransporters in both vertebrates and insects, are conserved in both aeCCC2 and Ncc83, suggesting a common mechanism of activation for the NaCCC2 and Na^+-K^+−$2Cl^-$ cotransporters (Delpire and Gagnon, 2011; Dowd and Forbush, 2003; Gagnon et al., 2006; Rodan, 2018).

In insect secretory epithelia, Na^+-K^+−$2Cl^-$ cotransporters carry ions across the basolateral membrane, contributing to secretion of salt (Beyenbach, 2003; Rodan et al., 2012). Expression patterns suggest different functions for NaCCC2s. In *Aedes aegypti*, the NaCCC2s are most highly expressed in tissues with absorptive functions. For example, aeCCC2 is highly expressed in the hindgut of adult and larval mosquitoes, whereas aeCCC3, a paralog of aeCCC2, is expressed abundantly in the anal papillae of larval mosquitoes (Durant et al., 2021; Durant and Donini, 2024; Hixson et al., 2022; Piermarini et al., 2017). An antibody against aeCCC2 stains the basolateral aspect of principal cells in the distal Malpighian tubules of larval and adult female *Aedes aegypti* (Duong et al., 2022), suggesting a possible role of aeCCC2 in transepithelial fluid secretion by tubules. An intriguing hypothesis is that aeCCC2 might contribute to the basolateral Na^+ conductance induced by cAMP (Hegarty et al., 1991; Kalsi et al., 2019; Sawyer and Beyenbach, 1985).

Expression of the gene that encodes Ncc83 has a somewhat different distribution than aeCCC2. According to the single-cell transcriptome data from Fly Cell Atlas, Ncc83 is most highly expressed in adult pylorus, visceral muscles of the midgut and crop, and Malpighian

tubule with detectable expression in midgut enterocytes as well (Li et al., 2022). In the Malpighian tubule, Ncc83 expression is restricted to principal cells of the lower Malpighian tubule and lower ureter, regions that reabsorb rather than secrete ions.

In addition to predicted roles in epithelia, Ncc83 and other insect cation-chloride cotransporters contribute to circadian rhythms by influencing electrophysiological properties and intracellular $[Cl^-]_i$ of clock neurons (Buhl et al., 2016; Eick et al., 2022; Rodan, 2024; Schellinger et al., 2022). Buhl and colleagues (2016) report that overexpression of Ncc83 depolarizes large ventral lateral neurons of *Drosophila melanogaster*, whereas knockdown caused them to hyperpolarize. (Ncc83 is referred to using the *NKCC* nomenclature in Buhl, et al. 2016.) These results are consistent with the electrogenic effects of NaCCC2s expressed in oocytes (Duong et al., 2022; Kalsi et al., 2019), particularly the Na^+-dependent depolarization of membrane potential. Na^+-K^+−$2Cl^-$ and K^+-Cl^- cotransporters also affect the circadian cycle by influencing $[Cl^-]_i$ and therefore modulating GABA signaling (Eick et al., 2022; Rodan, 2024; Schellinger et al., 2022). In some neurons, Ncc83 may also influence $[Cl^-]_i$, possibly through an indirect mechanism if Ncc83 is indeed chloride-independent like aeCCC2.

Prior work, mostly on the *Aedes aegypti* transporter aeCCC2, suggests that some functional properties of the NaCCC2s differ from other cation-chloride cotransporters (Duong et al., 2022; Kalsi et al., 2019). However, much less is known about other members of the NaCCC2 family, such as the *Drosophila melanogaster* transporter Ncc83. Also, assessing the function of NaCCC2s in neurons and secretory and absorptive epithelia requires better knowledge of their properties. Here we investigate the activation, inhibition, and other transport properties of Ncc83 and aeCCC2.

Methods

Exogenous expression in *Xenopus* oocytes.

Oocyte expression vectors for aeCCC2 (Vectorbase: AAEL009888) in pGH19 and Ncc83 (Flybase:cg31547) and Ncc69 (Flybase:cg4357) in pGEMHE were constructed previously (Duong et al., 2022; Kalsi et al., 2019). Vectors were linearized with NotI, purified (MinElute PCR purification, Qiagen), and cRNA was synthesized (mMESSAGE mMACHINE T7 Ultra kit, Thermo Fisher Scientific). Defolliculated oocytes were purchased from Ecocyte Bioscience, stored in OR3 at 18 °C, injected with 50 nl of cRNA in water (median amount injected = 44.5 ng, range = 13.5 – 142.5 ng) and studied 2–5 days after cRNA injection. We found similar responses across this range of injected cRNA. For example, the amount of cRNA injected did not significantly influence the response of Li^+ uptake to preincubation treatment (ANOVA, $p = 0.68$ for cRNA amount * preincubation interaction). Controls were injected with 50 nl of nuclease-free water.

Measurement of ion uptake.

Tracer ion uptake experiments were performed at room temperature on 24-well tissue culture plates as described previously (Kalsi et al., 2019). In a standard assay, oocytes were pre-incubated for 15 minutes in ND96 (isotonic) or ND96 diluted 50% with ultrapure

water (hypotonic) to stimulate cotransporter activity (Duong et al., 2022; Lytle and Forbush III, 1996; Ponce-Coria et al., 2008; Rodan, 2018), transferred for 30 minutes to isotonic uptake buffer containing 20 mM LiCl and 5 mM RbCl (uptake buffer also includes 63.2 mM choline chloride, 1 mM $MgCl_2$, 1.8 mM $CaCl_2$, 5 mM HEPES, pH 7.5, 195 mOsm/kg with choline chloride), and then washed three times for 2 min each in ice-cold choline-chloride wash buffer. For experiments in which intracellular cations and anions were evaluated (Tables 1 and 2), all washes were for ~15 seconds in ice-cold ultrapure water. In experiments testing activation or inhibition, 8-bromo-cAMP (8-Br-cAMP, 1 mM), ouabain (1 mM), and ethyl cinnamate (5.7 mM) were added to both the pre-incubation and uptake buffers. Ethyl cinnamate is a possible inhibitor of the NaCCC2s (Araújo et al., 2021). For [Li^+] curves, Li^+ was replaced by choline to maintain osmolarity.

After the washes, oocytes were transferred to ice-cold ultrapure water, then immediately to a 1.5 ml microfuge tube containing 1 ml of ultrapure water. Oocytes were lysed by pipetting them through a 200 μL tip, centrifuged for 10 minutes at 13,000 g to remove cell debris, and left overnight at room temperature to allow yolk lipids to separate from the aqueous phase. 200 μL aliquots were transferred to chromatography vials, avoiding the lipid layer.

Cation and anion concentrations of oocyte lysates were measured using high pressure ion chromatography (Integrion HPIC, AS-AP autosampler with 25 μL injection loop, CD conductivity detector; Thermo Fisher). Cations were separated using a Dionex CS12a column with 25 mM methanesulfonic acid eluent at a flow rate of 1 mL/min. Background conductivity was reduced with a CDRS-600 suppressor. Analysis of anions used a Dionex AS11-HC column, ADRS 600 suppressor, 30 mM KOH eluent, and a 1.5 ml/min flow rate. Data were collected with Chromeleon 7.2.8 software and ions were quantified by comparison to a standard curve of certified standards.

Electrophysiology methods.

To measure electrophysiological properties of *Xenopus* oocytes expressing aeCCC2 or Ncc83, we used a similar two-electrode voltage clamping (TEVC) approach as in Kalsi et al. (2019). Oocytes injected with H_2O were used as controls. In brief, each oocyte was initially held in a RC-1Z chamber (Warner Instruments, Hamden, CT) and bathed in flowing ND96 solution (4 ml/min). Two electrodes filled with 3M KCl were used to impale the oocytes for measuring membrane voltage (V_m) or membrane current (I_m). Once V_m of an oocyte stabilized, it was subjected to a voltage step protocol (controlled by the Clampex module of pCLAMP 9.0 Software, Molecular Devices) to measure the current (I)-voltage (V) relationship across a range of V_m values (−140 mV to + 40 mV in 20 mV steps). Whole oocyte conductance was calculated as the I-V curve slope from −140 mV to +40 mV. To determine if intracellular cAMP elevation affected electrophysiological properties of the oocytes, flow to the chamber was first stopped to maintain a standing bath volume of ~750 μl. Next, 7.5 μl of 100 mM 8-bromo-cAMP (8-Br-cAMP) dissolved in H_2O was added to the bath with gentle mixing, resulting in a final concentration of ~1 mM 8-Br-cAMP. I-V plots were then recorded at 15 min and 30 min after adding 8-Br-cAMP. The high cost of 8-Br-cAMP and chronic nature of these experiments precluded our use of a running bath. After the I-V plot at 30 min, flow of ND96 to bath returned.

In some oocytes, we also measured Na^+-dependent I_m values of the oocytes before and after 8-Br-cAMP treatment. In these oocytes, after the initial I-V relationship was recorded in ND96 (96 mM Na^+) and before the flow to the bath was stopped, the solution was switched to a 1000-fold lower Na^+ buffer (ND0.096) where 99.9% of the Na^+ was replaced with N-methyl-D-glucamine ($NMDG^+$). After ~40 s exposure to ND0.096, another I-V relationship was recorded. The difference in I_m values between the I-V plots allowed for determination of Na^+-dependent currents at each voltage step. Following the ND0.096 exposure, the buffer was returned to ND96 and V_m was allowed to restabilize before stopping the bath for 8-Br-cAMP treatment. After 30 min of 8-Br-cAMP treatment, the I-V relationships in ND96 and ND0.096 were repeated to determine how elevated intracellular cAMP affected Na^+-dependent currents.

Analysis and statistics.

Prior to analysis of tracer ion experiments, we removed data from oocytes with K^+_i content less than 15 nmol, which corresponds to a concentration of ~15 mM if oocyte volume is 1 μL. Oocytes with these very low $[K^+]_i$ are probably unhealthy; for example, early *Xenopus* embryos with $[K^+]_i$ less than 60 mM are not viable (Gillespie, 1983). This resulted in 12% of oocytes considered outliers and not being included in the final analysis. Also, two oocytes (one expressing aeCCC2 and one expressing Ncc83) with calculated Li^+ uptake rates more than twice the V_{max} (above 500 pmol/min) were considered outliers and not included in the analysis of $[Li^+]$ dependence of Li^+ uptake. Statistical comparisons were made using ANOVA tests with Tukey's post-hoc analysis of individual differences. Unless otherwise noted, p-values are from Tukey's post-hoc comparisons between water-injected and cRNA-injected oocytes or between treatment conditions for oocytes injected with the same cRNA. Values reported in the text are means ± sd unless otherwise noted.

Results

NaCCC2s transport Li^+ but not Rb^+.

In preliminary experiments, we compared Li^+ and Rb^+ uptake rates in oocytes injected with cRNA encoding Ncc69, Ncc83, or aeCCC2 to water-injected controls. Following hypotonic or isotonic pre-incubation, Li^+ uptake rates were approximately three fold greater in oocytes expressing Ncc83 or aeCCC2 than in oocytes expressing Ncc69 or in water-injected controls (Supplemental Figure 1A and 2A; ANOVA, $p < 0.01$, n = 15–64 oocytes per treatment). In contrast, Rb^+ uptake rates were not different between water-injected controls and those injected with cRNA (Supplemental Figure 1B and 2B). These findings are consistent with prior work showing that oocytes expressing aeCCC2 demonstrate increased Na^+ and Li^+ dependent currents and Li^+ uptake, but no difference from control in K^+ dependent currents and Rb^+ uptake (Kalsi et al., 2019). However, the effect of hypotonic swelling cannot be determined from these data because hypotonic and isotonic pre-incubations were performed in separate experiments.

Hypotonic swelling activates NaCCC2 Li^+ uptake.

To examine the activation of NaCCC2s by hypotonic swelling, we measured the Li^+ uptake rate of oocytes following exposure to hypotonic or isotonic preincubation. Li^+ uptake rates

of control water-injected oocytes were not significantly different between isotonic and hypotonic exposure (ANOVA, p=0.78) (Fig. 1A). In contrast, aeCCC2-injected oocytes had Li^+ uptake rates of 88.0 ± 32.3 pmol/min following hypotonic pre-incubation, an 87% increase over uptake following isotonic pre-incubation (ANOVA, p=0.03). Similarly, Ncc83 transport was also activated by hypotonic exposure (Fig. 1A). Li^+ uptake rates in Ncc83-injected oocytes were 41.8 ± 14.1 pmol/min following isotonic preincubation and increased to 100.3 ± 41.7 pmol/min following hypotonic preincubation (ANOVA, $p<0.01$). Rb^+ uptake rate was not different among oocytes expressing Ncc69, aeCCC2, or Ncc83, but was somewhat greater following hypotonic pre-incubation, possibly due to activation of the Na^+-K^+-ATPase by swelling (ANOVA, p = 0.010; Fig. 1B). These data show that Li^+ uptake by aeCCC2 and Ncc83 is activated by hypotonic swelling, consistent with prior work on the effects of swelling on V_m (Duong et al., 2022).

Oocyte anion and cation content:

In a separate set of experiments, we measured cation and anion content of oocytes after flux assays with hypotonic and isotonic preincubations (Tables 1 and 2). Cell Li^+ content followed the same pattern as Fig 1A (Table 1). Li^+ content in aeCCC2 and Ncc83 was greater than in water-injected controls (ANOVA, $p < 0.01$) and increased in response to hypotonic preincubation (ANOVA, $p < 0.01$). Na^+ content was slightly lower following hypotonic pre-incubation in aeCCC2 and Ncc83 oocytes and water-injected controls (p = 0.046). The content of other non-tracer cations (K^+, Mg^{2+}, and Ca^{2+}) did not differ between hypotonic and isotonic pre-incubation, but did show small differences among aeCCC2, Ncc83, and water-injected oocytes. In particular, Mg^{2+} and Ca^{2+} levels were 23–34% higher in aeCCC2 oocytes compared to than water injected controls (ANOVA, $p < 0.01$).

Chloride content did not differ between water-injected controls and oocytes expressing aeCCC2 and Ncc83, and was not different between isotonic and hypotonic preincubation (Table 2). However, phosphate content was lower in oocytes expressing aeCCC2 compared to water-injected controls following both isotonic and hypotonic preincubation (Table 2, p = 0.028).

Response of intracellular Na^+ and Li^+ uptake to ouabain.

If the NaCCC2s transport Na^+, then expression of aeCCC2 and Ncc83 in oocytes would tend to increase intracellular [Na^+]. However, cellular Na^+ content of aeCCC2 or Ncc83 oocytes following flux assays did not differ from controls. One possibility is that active efflux of Na^+ through the Na^+-K^+-ATPase might counter Na^+ uptake through the aeCCC2 or Ncc83. Thus, we measured internal content of cations in the presence of the Na^+-K^+-ATPase inhibitor ouabain. In the presence of ouabain in an isotonic ND96 solution, water-injected oocytes had internal Na^+ content of 12.6 ± 1 nmol/cell (Fig. 2A). Following the same treatment, aeCCC2-injected oocytes had approximately 50% higher Na^+ concentrations of 18.8 ± 4.9 nmol (ANOVA, p= 0.036), whereas Na^+ content of oocytes expressing Ncc83 was not different than controls (ANOVA, p = 0.855). After hypotonic pre-incubation in the presence of ouabain, water-injected oocytes had Na^+ content of 11.9 ± 2 nmol; Na^+ content of aeCCC2-expressing oocytes was approximately 64% greater than controls (19.5 ± 2.5mM; ANOVA, p = 0.005). Na^+ content of oocytes expressing Ncc83 was ~45% greater than

controls after hypotonic pre-incubation, although this difference fell just short of statistical significance (17.2 ± 3.5mM; ANOVA, p = 0.051). Similar to findings in the absence of ouabain (Table 1), differences in Na^+ content between hypotonic and isotonic incubation were not significantly different (Fig 2A, ANOVA, p=0.18).

In a separate experiment, Li^+ uptake was measured in oocytes in the presence of 1 mM ouabain (Fig. 2B). Li^+ uptake rate of oocytes expressing aeCCC2 and Ncc83 were both greater than water-injected controls (ANOVA, $p < 0.01$). In contrast to experiments in the absence of ouabain (Fig 1A), no significant differences were measured between isotonic and hypotonic pre-incubation although there was a trend towards increased Li^+ uptake after hypotonic pre-incubation.

Li^+ uptake by NaCCC2s is concentration dependent and saturable.

To examine the apparent affinities of NaCCC2s for transported cations, Li^+ uptake was measured in increasing concentrations of extracellular Li^+. As Li^+ concentrations increased, Ncc83 and aeCCC2-mediated Li^+ uptake rate plateaued (Fig. 3), following a curve consistent with simple Michaelis-Menten kinetics. The K_m for Li^+ uptake by aeCCC2 was 20.10 ± 11.50 mM (n = 4), and the K_m for Li^+ uptake by Ncc83 was 10.61 ± 4.85 mM (n = 4).

cAMP has different effects in aeCCC2 and Ncc83 injected oocytes.

Li^+ uptake rate of oocytes expressing Ncc83 increased in response to 1 mM 8-Br-cAMP (ANOVA, p=0.002) but 8-Br-cAMP did not stimulate Li^+ uptake in oocytes expressing aeCCC2 (ANOVA, p=0.96) (Fig. 4A). In contrast to other experiments, oocytes expressing aeCCC2 had a higher Rb^+ uptake rate than the water control (ANOVA, p=0.001). Rb^+ uptake was also stimulated by cAMP exposure in oocytes expressing aeCCC2 (ANOVA, p=0.006; Fig. 4B).

Ethyl cinnamate does not affect NaCCC2 activity.

Cinnamic acid derivatives, including ethyl cinnamate, are possible inhibitors of aeCCC2 (Araújo et al., 2021). Neither Li^+ uptake rate nor Rb^+ uptake rates were affected by 5.7 mM ethyl cinnamate following isotonic or hypotonic pre-incubation. (Figure 5, ANOVA, $p > 0.05$).

Electrophysiology—We next measured the effects of increased intracellular cAMP on the electrophysiology of *Xenopus* oocytes expressing aeCCC2. As shown in Fig. 6A, treatment of an aeCCC2 oocyte with 1 mM 8-Br-cAMP (arrow) led to a slow depolarization of V_m by ~10 mV over 30 min. In contrast, treatment of a H_2O-injected oocyte showed a hyperpolarization of ~5 mV over 30 min (Fig. 6B). On average, 8-Br-cAMP induced a significant depolarization of V_m by 9.57 ± 1.57 mV (mean ± SEM; n = 7) in aeCCC2 oocytes, which was significantly different than the effects of 8-Br-cAMP on V_m in H_2O-injected oocytes (−2.10 ± 2.79 mV; n = 7; $P < 0.01$, t-test).

We also recorded the I-V relationships of the oocytes immediately before and at two time points after adding 8-Br-cAMP (15 min and 30 min). Given that the effects at 15

min were typically intermediate, we focused on the 30 min time point when the effects appeared maximal. Figure 6C shows the mean (± SEM) I-V relationships of aeCCC2 and H_2O-injected oocytes before (pre) and 30 min after treatment with 8-Br-cAMP (30 min). The ‘pre’ mean I-V relationship of aeCCC2 oocytes was noticeably steeper than that of H_2O-injected oocytes (Fig. 6C), consistent with observations in our earlier study (Kalsi et al., 2019). As such, the ‘pre’ mean slope conductance of aeCCC2 oocytes was significantly greater than that of H_2O-injected oocytes (Fig. 6D). The ‘30 min’ I-V relationships of aeCCC2 oocytes showed increased steepness compared to the ‘pre’, whereas those of H_2O-injected oocytes were similar. Consistent with these observations, the ‘30 min’ mean slope conductance of aeCCC2 oocytes significantly increased compared to ‘pre’, whereas that of H_2O-injected cells did not. As such, the ‘30 min’ mean slope conductance of aeCCC2 oocytes was significantly greater than that of H_2O-injected oocytes.

To determine if 8-Br-cAMP also altered the electrophysiology of NCC83 oocytes, we performed similar experiments using independent batches of oocytes. As shown in Fig. 7A, similar to aeCCC2, treatment of an NCC83 oocyte with 1 mM 8-Br-cAMP led to a slow depolarization of V_m by ~18 mV over 30 min. However, treatment of a H_2O-injected oocyte showed a similar slow depolarization of ~10 mV over 30 min (Fig. 7B). Although on average the depolarization of V_m induced by 8-Br-cAMP in NCC83 oocytes (17.04 ± 4.06 mV, mean ± SEM; n = 6) was larger than that in H_2O-injected oocytes (9.59 ± 1.73; n = 8), the means were not significantly different (P = 0.08, t-test). Figure 7C shows the average I-V relationships of NCC83 and H_2O-injected oocytes before (pre) and 30 min after treatment with 8-Br-cAMP (30 min). The ‘pre’ mean I-V relationship of NCC83 oocytes was slightly steeper than that of H_2O-injected oocytes. Consistent with this appearance, the ‘pre’ mean slope conductance of NCC83 oocytes was similar to that of H_2O-injected oocytes (Fig. 7D). However, the ‘30 min’ mean I-V relationship was remarkably steeper compared to that of the ‘pre’ in NCC83 oocytes, whereas those of H_2O-injected oocytes were less affected (Fig. 7C). As such, the ‘30 min’ mean slope conductance of NCC83 oocytes was significantly larger than that of the ‘pre’, whereas those of H_2O-injected oocytes were similar (Fig. 7D). Likewise, the ‘30 min’ mean slope conductance of NCC83 oocytes was significantly greater than that of H_2O-injected oocytes.

To generate insights as to whether the enhanced conductance of aeCCC2 and NCC83 oocytes after 8-Br-cAMP treatment was associated with increased Na^+-currents, we also measured the ‘pre’ and ‘30 min’ Na^+-dependent currents at the extreme ends of the I-V plots (i.e., −140 mV and +40 mV, where inward and outward currents are maximal, respectively) in a subset of oocytes. In aeCCC2 oocytes, when clamped at −140 mV, the ‘pre’ mean Na^+-dependent inward currents were significantly greater than those of H_2O-injected oocytes (Fig. 8A), consistent with earlier observations (Kalsi et al., 2019). The ‘30 min’ mean inward Na^+-dependent currents of aeCCC2 oocytes was significantly greater than that of ‘pre’, whereas those of H_2O-injected oocytes were similar (Fig. 8A). As such, the ‘30 min’ mean inward Na^+-dependent current of aeCCC2 oocytes was significantly greater than that of H_2O-injected oocytes. Similar effects and patterns were observed in aeCCC2 and H_2O-injected oocytes for the Na^+-dependent outward currents at +40 mV with the exception that the ‘pre’ mean outward currents were not significantly different between aeCCC2 and

H_2O-injected oocytes (Fig. 8B); the 'pre' similarity of outward currents is consistent with observations made in a previous study (Kalsi et al., 2019).

In NCC83 oocytes, when clamped at −140 mV, the 'pre' mean Na^+-dependent inward currents were similar to those of H_2O-injected oocytes (Fig. 8C). The '30 min' mean inward Na^+-dependent currents of NCC83 oocytes was significantly greater than that of 'pre', whereas those of H_2O-injected oocytes were similar (Fig. 8C). As such, the '30 min' mean inward Na^+-dependent current of NCC83 oocytes was significantly greater than that of H_2O-injected oocytes (Fig. 8C). Similar effects and patterns were observed in NCC83 and H_2O-injected oocytes for the Na^+-dependent outward currents at +40 mV (Fig. 8D).

Discussion

Our results show that uptake of Li^+ (a tracer for Na^+) in oocytes expressing aeCCC2 is saturable (Figure 3A) and activated by hypotonic swelling (Figure 1A), confirming with tracer flux assays findings from prior electrophysiology experiments. We also report the characterization of Ncc83 by tracer uptake assays. Similar to findings with aeCCC2, oocytes expressing Ncc83 transport Li^+ but not Rb^+ at a higher rate than water-injected controls (Figure 1A). Ncc83 also resembles aeCCC2 in its saturation at higher [Li^+] and activation by hypotonic swelling (Figures 1A and 3B). Finally, our results in both tracer assays and electrophysiology show that cAMP activates Ncc83 and possibly aeCCC2 (Figures 4 and 6–8), albeit to a smaller extent than activation by hypotonic swelling.

Activation by hypotonic swelling.

In oocytes expressing aeCCC2 or Ncc83, membrane hyperpolarization following removal of Na^+ was increased following a 10 minute exposure to hypotonic swelling (Duong et al., 2022). Here, we show that Li^+ uptake is also activated by hypotonic exposure in oocytes expressing both aeCCC2 and Ncc83 (Figure 1A). This activation is probably due to phosphorylation of the transporters by the WNK-SPAK/OSR1 kinase cascade in response to reduction of $[Cl^-]_i$, a well-documented mechanism in vertebrate and insect Na^+-K^+-Cl^- cotransporters (Dowd and Forbush, 2003; Murillo-de-Ozores et al., 2020; Rodan, 2018; Wu et al., 2014). Our measurements indicate that intracellular Cl^- content is the same following hypotonic and isotonic pre-incubation (Table 2). Thus, $[Cl^-]_i$ must decrease as oocytes swell during hypotonic exposure. Moreover, Ncc83 and aeCCC2 have phosphorylation sites for SPAK (Duong et al., 2022). This shared regulatory mechanism suggests that the NaCCC2s might be active simultaneously with Na-K-2Cl cotransporters in insect epithelia.

In the presence of ouabain, Li^+ uptake was increased in oocytes expressing aeCCC2 and Ncc83 compared to water-injected controls (Figure 2B). Thus, ouabain does not inhibit activity of aeCCC2 and Ncc83. In these experiments, no differences in Li^+ uptake were measured between isotonic and hypotonic pre-incubation, possibly because inhibition of Na-K-ATPase in ouabain-treated cells leads to cell swelling in cells preincubated in both isotonic and hypotonic saline. Thus, transport may already be at least partly activated in the isotonic condition.

Intracellular ion content.

The cation and anion contents reported in Table 1 were assessed in oocytes following flux assays during which oocytes were exposed first to hypotonic or isotonic preincubation and then to assay solutions in which Na^+ was replaced by Li^+ and choline. Thus, they represent ion content following the flux assays, which may differ from levels in resting conditions. Assuming an oocyte volume of 1 μL, the measured values for Na^+ and K^+ content correspond to concentrations of 10–20 mM for Na^+ and 59–77 mM for K^+ (Figure 2A, Table 1). These values are within the ranges measured in other studies (Sobczak et al., 2010), but the calculated concentrations of Na^+ are somewhat greater than measurements of Na^+ activity in *Xenopus* oocytes by ion-selective microelectrode (Chintapalli et al., 2015). This discrepancy may reflect that some Na^+ is sequestered and therefore not measured by microelectrodes but detected by cation chromatography of lysates. In a study of *Bufo bufo* oocytes, Na^+ concentrations assessed by flame photometry of whole-cell lysates were substantially greater (33.7 mM) than measurements made by microprobe (Dick, 1978). Altogether, the small differences in ion levels between oocytes suggest that the differences in Li^+ uptake are not indirect results of differing cation and anion levels (Table 1 and 2).

Following exposure to ouabain, aeCCC2-injected *Xenopus* oocytes contained higher Na^+ content than water-injected controls, suggesting that aeCCC2 imports Na^+ under resting conditions (Figure 2A). In contrast, no significant difference in Na^+ content was found between oocytes expressing NaCCC2s and controls following tracer flux assays in which ouabain was not present (Table 1). Presumably, increased Na-K-ATPase activity compensates for the Na^+ influx in the absence of ouabain. A tendency towards increased membrane Na^+ permeability is consistent with the depolarized membrane potential of oocytes expressing aeCCC2 (Duong et al., 2022; Kalsi et al., 2019). This result is also consistent with findings of this study including greater Li^+ uptake in oocytes expressing aeCCC2 compared to controls following isotonic ND96 preincubation (Fig. 1A) as well as enhanced slope conductance and inward Na^+ currents of aeCCC2 oocytes compared to H_2O prior to cAMP treatment (Figs. 6 and 8A–B). Also, an increased Na^+ conductance could explain the decrease in intracellular phosphate in oocytes expressing aeCCC2 (Table 2), because an alternative pathway for inward Na^+ movement could decrease phosphate uptake through endogenous Na^+-phosphate cotransporters of Xenopus oocytes (Eckard and Passow, 1987). In contrast, in the presence of ouabain, oocytes expressing Ncc83 do not have significantly greater Na^+ content than water-injected controls (Figure 2A). This finding is consistent with electrophysiology results showing both slope conductance and Na^+-dependent inward currents of Ncc83 is similar to H_2O prior to cAMP exposure (Figs. 7 and 8C–D).

Dependence of Li^+ uptake on [Li^+].

Li^+ uptake saturated at increasing concentration of Li^+ in oocytes expressing both aeCCC2 and Ncc83, with apparent affinities (K_m) in the range of 10–20 mM (Figure 3). This finding is consistent with the dependence of membrane currents on [Na^+] in oocytes expressing aeCCC2 voltage-clamped at −60 mV (Duong et al., 2022). Slightly lower affinities (higher K_m) for Li^+ uptake in the current experiment than in prior work for Na^+-dependent currents (K_m ~ 5mM) could be due to differences between Li^+ and Na^+ affinities of the transport

proteins or due to technical differences between the experiments. Because no specific inhibitor of the NaCCC2s has been identified, we cannot differentiate between Li^+ uptake by aeCCC2 and Ncc83 and uptake through endogenous pathways that could also depend on [Li^+]. Endogenous Li^+ uptake in water-injected controls is quite low compared to oocytes expressing Ncc83 and aeCCC2 at 20 mM external [Li^+] (Figure 3A), but probably contributes to a relatively greater portion of total Li^+ uptake at higher external [Li^+] as the transporters saturate. Although these experimental challenges could affect the precise determination of K_m, the saturation of aeCCC2 and Ncc83 at increasing [Li^+] with relatively high affinity indicates a carrier-like rather than channel-like transport mechanism.

The functional consequences of Na^+/Li^+ affinities of Ncc83 and aeCCC2 remain difficult to predict without information about whether they are localized to apical or basolateral membranes in tissues such as hindgut where they are most highly expressed. Moreover, although we currently have no evidence for cotransport or exchange of other substrates with Na^+ through Ncc83 or aeCCC2, we can't rule out the possibility. Fluid secreted by adult *Drosophila melanogaster* Malpighian tubules has a [Na^+] of approximately 20 mM (Naikkhwah and O'Donnell, 2011; Rodan et al., 2012); a wider range of [Na^+] has been measured in hemolymph (~45–135 mM) (MacMillan and Hughson, 2014; Naikkhwah and O'Donnell, 2011). Thus, the [Na^+] on both sides of the *Drosophila* hindgut epithelium are likely to be above the K_m for Na^+, and at levels that would saturate extracellular binding sites for transport on the basolateral but possibly not on the apical side of the epithelium.

cAMP.

Our results show that increasing intracellular cAMP activates aeCCC2 and Ncc83, although this effect is more consistently observed for Ncc83 than aeCCC2. Treatment with 8-Br-cAMP significantly increased Li^+ uptake in oocytes expressing Ncc83, but not aeCCC2 (Figure 4A). One explanation for this difference between Ncc83 and aeCCC2 is that aeCCC2 may be more active in resting conditions than Ncc83 as discussed earlier (under Intracellular cation and ion content), leaving less opportunity for activation by cAMP. Another possible explanation is differences in the predicted protein kinase A phosphorylation sites on each protein. According to analysis of phosphorylation sites at ScanSite 4.0 (medium stringency, scansite.mit.edu), Ncc83 has three predicted PKA sites on the N-terminus but aeCCC2 has only two (Obenauer et al., 2003). Results from electrophysiology experiments also show activation of NaCCC2s by cAMP. Slope conductances and Na^+-dependent currents were greater following treatment with 8-Br-cAMP in both Ncc83 and aeCCC2.

Surprisingly, aeCCC2-injected oocytes demonstrate increased uptake of Rb^+ in response to cAMP activation (Fig 4B). This Rb^+ uptake is probably not through aeCCC2, since no increase of Rb^+ uptake in oocytes expressing aeCCC2 was measured in other experiments. One possibility is that this increased Rb^+ uptake is mediated by the Na^+-K^+-ATPase, and that oocytes expressing aeCCC2 have increased levels of Na-K-ATPase expression to counter the baseline Na^+ influx through aeCCC2.

Intriguingly, the electrophysiological effects induced by 8-Br-cAMP on aeCCC2 oocytes resemble those observed on the basolateral membranes of principal cells in mosquito

Malpighian tubules (Beyenbach and Masia, 2002; Coast et al., 2005; Sawyer and Beyenbach, 1985). Similar to the basolateral membrane of principal cells, increases of intracellular cAMP in aeCCC2 oocytes depolarized the membrane potential and enhanced the membrane Na^+-conductance. Together with the localization of aeCCC2 immunoreactivity to the basal aspect of principal cells in the distal segment of adult female mosquito Malpighian tubules (Duong et al., 2022), these results suggest that aeCCC2 might contribute in part to the cAMP-activated Na^+-conductance in principal cells described by others (Beyenbach and Masia, 2002; Coast et al., 2005; Sawyer and Beyenbach, 1985). One important difference is that in Malpighian tubules the cAMP-stimulated Na^+ conductance is blocked by amiloride, whereas the Na^+-conductance of aeCCC2 oocytes appears to be insensitive to amiloride (Kalsi et al., 2019).

Summary

Evidence from prior work indicates that the insect NaCCC2s, in contrast other cation-chloride cotransporters, carry charge across membranes (Duong et al., 2022; Kalsi et al., 2019). The findings of this paper both support and extend this surprising conclusion. Electrophysiology and tracer flux results are well aligned within this study and between this study and previous work. Moreover, results are similar (but not identical) in oocytes expressing aeCCC2 and Ncc83. As expected, the NaCCC2s share some properties with the closely related vertebrate and insect Na^+-K^+−$2Cl^-$ cotransporters, including activation by hypotonic swelling and saturable transport of Na^+/Li^+. Although the specific functions of NaCCC2s in insect epithelia remain to be determined, activation of NaCCC2s by cAMP supports the hypothesis of roles in salt secretion by Malpighian tubules (Coast et al., 2005; Duong et al., 2022; Kalsi et al., 2019; Sawyer and Beyenbach, 1985). In summary, the functional differences between NaCCC2s and Na^+-K^+−$2Cl^-$ cotransporters offer opportunities for comparative structure-function studies, suggest novel roles for NaCCC2s in transporting epithelia and other cells, and could be the basis of new insect-control strategies.

Supplementary Material

Refer to Web version on PubMed Central for supplementary material.

Acknowledgements

Funding for this research was provided by the National Institute of Health: R15GM139088, State and Federal funds appropriated to the OARDC of the Ohio State University, and Kenyon College. The content is solely the responsibility of the authors and does not necessarily represent the official views of the National Institutes of Health. We thank Dr. Kathy Gillen for helpful comments on the manuscript. Plasmids containing ORFs of Drosophila Ncc69 and Ncc83 were obtained from the Drosophila Genomic Resource Center, Bloomington, IN.

References

Araújo MO, Pérez-Castillo Y, Oliveira LHG, Nunes FC, Sousa D.P. de, 2021. Larvicidal Activity of Cinnamic Acid Derivatives: Investigating Alternative Products for Aedes aegypti L. Control. Molecules 26. 10.3390/molecules26010061

Beyenbach KW, 2003. Transport mechanisms of diuresis in Malpighian tubules of insects. J Exp Biol 206, 3845–3856. 10.1242/jeb.00639 [PubMed: 14506220]

Beyenbach KW, Masia R, 2002. Membrane conductances of principal cells in Malpighian tubules of Aedes aegypti. J. Insect Physiol 48, 375–386. 10.1016/S0022-1910(02)00057-4 [PubMed: 12770112]

Buhl E, Bradlaugh A, Ogueta M, Chen K-F, Stanewsky R, Hodge JJL, 2016. Quasimodo mediates daily and acute light effects on Drosophila clock neuron excitability. Proc. Natl. Acad. Sci 113, 13486–13491. 10.1073/pnas.1606547113 [PubMed: 27821737]

Chew TA, Orlando BJ, Zhang J, Latorraca NR, Wang A, Hollingsworth SA, Chen D-H, Dror RO, Liao M, Feng L, 2019. Structure and mechanism of the cation–chloride cotransporter NKCC1. Nature 572, 488–492. 10.1038/s41586-019-1438-2 [PubMed: 31367042]

Coast GM, Garside CS, Webster SG, Schegg KM, Schooley DA, 2005. Mosquito natriuretic peptide identified as a calcitonin-like diuretic hormone in Anopheles gambiae (Giles). J. Exp. Biol 208, 3281–3291. 10.1242/jeb.01760 [PubMed: 16109890]

Delpire E, Gagnon KB, 2011. Kinetics of hyperosmotically stimulated Na-K-2Cl cotransporter in Xenopus laevis oocytes. Am. J. Physiol.-Cell Physiol 301, C1074–C1085. 10.1152/ajpcell.00131.2011 [PubMed: 21775703]

Delpire E, Guo J, 2020. Cryo-EM structures of DrNKCC1 and hKCC1: a new milestone in the physiology of cation-chloride cotransporters. Am. J. Physiol.-Cell Physiol 318, C225–C237. 10.1152/ajpcell.00465.2019 [PubMed: 31747317]

Dowd BFX, Forbush B, 2003. PASK (Proline-Alanine-rich STE20-related Kinase), a Regulatory Kinase of the Na-K-Cl Cotransporter (NKCC1). J Biol Chem 278, 27347–27353. 10.1074/jbc.M301899200 [PubMed: 12740379]

Duong PC, McCabe TC, Riley GF, Holmes HL, Piermarini PM, Romero MF, Gillen CM, 2022. Sequence analysis and function of mosquito aeCCC2 and Drosophila Ncc83 orthologs. Insect Biochem. Mol. Biol 143, 103729. 10.1016/j.ibmb.2022.103729

Durant AC, Donini A, 2024. Ammonia transport in the excretory system of mosquito larvae (Aedes aegypti): Rh protein expression and the transcriptome of the rectum. Comp. Biochem. Physiol. A. Mol. Integr. Physiol 294, 111649. 10.1016/j.cbpa.2024.111649

Durant AC, Grieco Guardian E, Kolosov D, Donini A, 2021. The transcriptome of anal papillae of Aedes aegypti reveals their importance in xenobiotic detoxification and adds significant knowledge on ion, water and ammonia transport mechanisms. J. Insect Physiol 132, 104269. 10.1016/j.jinsphys.2021.104269

Eckard P, Passow H, 1987. Sodium-dependent and sodium-independent phosphate uptake by full-grown, prophase-arrested oocytes of Xenopus laevis before and after progesterone-induced maturation. Cell Biol. Int. Rep 11, 349–358. 10.1016/0309-1651(87)90001-4 [PubMed: 3038342]

Eick AK, Ogueta M, Buhl E, Hodge JJL, Stanewsky R, 2022. The opposing chloride cotransporters KCC and NKCC control locomotor activity in constant light and during long days. Curr. Biol 32, 1420–1428.e4. 10.1016/j.cub.2022.01.056 [PubMed: 35303416]

Gagnon KBE, England R, Delpire E, 2006. Characterization of SPAK and OSR1, Regulatory Kinases of the Na-K-2Cl Cotransporter. Mol Cell Biol 26, 689–698. [PubMed: 16382158]

Gillespie JI, 1983. The distribution of small ions during the early development of Xenopus laevis and Ambystoma mexicanum embryos. J. Physiol 344, 359–377. 10.1113/jphysiol.1983.sp014945 [PubMed: 6655587]

Hartmann A-M, Tesch D, Nothwang HG, Bininda-Emonds ORP, 2014. Evolution of the Cation Chloride Cotransporter Family: Ancient Origins, Gene Losses, and Subfunctionalization through Duplication. Mol. Biol. Evol 31, 434–447. 10.1093/molbev/mst225 [PubMed: 24273324]

Hegarty JL, Zhang B, Pannabecker TL, Petzel DH, Baustian MD, Beyenbach KW, 1991. Dibutyryl cAMP activates bumetanide-sensitive electrolyte transport in Malpighian tubules. Am. J. Physiol. - Cell Physiol 261, C521–C529.

Hixson B, Bing X-L, Yang X, Bonfini A, Nagy P, Buchon N, 2022. A transcriptomic atlas of Aedes aegypti reveals detailed functional organization of major body parts and gut regional specializations in sugar-fed and blood-fed adult females. eLife 11, e76132. 10.7554/eLife.76132

Kalsi M, Gillen C, Piermarini PM, 2019. Heterologous Expression of Aedes aegypti Cation Chloride Cotransporter 2 (aeCCC2) in Xenopus laevis Oocytes Induces an Enigmatic Na+/Li+ Conductance. Insects 10, 71. 10.3390/insects10030071 [PubMed: 30875796]

Li H, Janssens J, De Waegeneer M, Kolluru SS, Davie K, Gardeux V, Saelens W, David FPA, Brbić M, Spanier K, Leskovec J, McLaughlin CN, Xie Q, Jones RC, Brueckner K, Shim J, Tattikota SG, Schnorrer F, Rust K, Nystul TG, Carvalho-Santos Z, Ribeiro C, Pal S, Mahadevaraju S, Przytycka TM, Allen AM, Goodwin SF, Berry CW, Fuller MT, White-Cooper H, Matunis EL, DiNardo S, Galenza A, O'Brien LE, Dow JAT, FCA Consortium§, Jasper H, Oliver B, Perrimon N, Deplancke B, Quake SR, Luo L, Aerts S, Agarwal D, Ahmed-Braimah Y, Arbeitman M, Ariss MM, Augsburger J, Ayush K, Baker CC, Banisch T, Birker K, Bodmer R, Bolival B, Brantley SE, Brill JA, Brown NC, Buehner NA, Cai XT, Cardoso-Figueiredo R, Casares F, Chang A, Clandinin TR, Crasta S, Desplan C, Detweiler AM, Dhakan DB, Donà E, Engert S, Floc'hlay S, George N, González-Segarra AJ, Groves AK, Gumbin S, Guo Y, Harris DE, Heifetz Y, Holtz SL, Horns F, Hudry B, Hung R-J, Jan YN, Jaszczak JS, Jefferis GSXE, Karkanias J, Karr TL, Katheder NS, Kezos J, Kim AA, Kim SK, Kockel L, Konstantinides N, Kornberg TB, Krause HM, Labott AT, Laturney M, Lehmann R, Leinwand S, Li J, Li JSS, Li Kai, Li Ke, Li L, Li T, Litovchenko M, Liu H-H, Liu Y, Lu T-C, Manning J, Mase A, Matera-Vatnick M, Matias NR, McDonough-Goldstein CE, McGeever A, McLachlan AD, Moreno-Roman P, Neff N, Neville M, Ngo S, Nielsen T, O'Brien CE, Osumi-Sutherland D, Özel MN, Papatheodorou I, Petkovic M, Pilgrim C, Pisco AO, Reisenman C, Sanders EN, dos Santos G, Scott K, Sherlekar A, Shiu P, Sims D, Sit RV, Slaidina M, Smith HE, Sterne G, Su Y-H, Sutton D, Tamayo M, Tan M, Tastekin I, Treiber C, Vacek D, Vogler G, Waddell S, Wang W, Wilson RI, Wolfner MF, Wong Y-CE, Xie A, Xu J, Yamamoto S, Yan J, Yao Z, Yoda K, Zhu R, Zinzen RP, 2022. Fly Cell Atlas: A single-nucleus transcriptomic atlas of the adult fruit fly. Science 375, eabk2432. 10.1126/science.abk2432

Liu S, Chang S, Han B, Xu L, Zhang M, Zhao C, Yang W, Wang F, Li J, Delpire E, Ye S, Bai X, Guo J, 2019. Cryo-EM structures of the human cation-chloride cotransporter KCC1. Science 366, 505–508. 10.1126/science.aay3129 [PubMed: 31649201]

Lytle C, Forbush III B, 1996. Regulatory phosphorylation of the secretory Na-K-Cl cotransporter: modulation by cytoplasmic Cl. Amer J Physiol Cell Physiol 39 270, C437–48.

MacMillan HA, Hughson BN, 2014. A high-throughput method of hemolymph extraction from adult Drosophila without anesthesia. J. Insect Physiol 63, 27–31. 10.1016/j.jinsphys.2014.02.005 [PubMed: 24561358]

Murillo-de-Ozores AR, Chávez-Canales M, de los Heros P, Gamba G, Castañeda-Bueno M, 2020. Physiological Processes Modulated by the Chloride-Sensitive WNK-SPAK/OSR1 Kinase Signaling Pathway and the Cation-Coupled Chloride Cotransporters. Front. Physiol 11, 1353. 10.3389/fphys.2020.585907

Naikkhwah W, O'Donnell MJ, 2011. Salt stress alters fluid and ion transport by Malpighian tubules of *Drosophila melanogaster*: evidence for phenotypic plasticity. J. Exp. Biol 214, 3443–3454. 10.1242/jeb.057828 [PubMed: 21957108]

Obenauer JC, Cantley LC, Yaffe MB, 2003. Scansite 2.0: proteome-wide prediction of cell signaling interactions using short sequence motifs. Nucleic Acids Res 31, 3635–3641. 10.1093/nar/gkg584 [PubMed: 12824383]

Payne JA, 2012. Molecular Operation of the Cation Chloride Cotransporters: Ion Binding and Inhibitor Interaction. Curr. Top. Membr 70, 215–237. 10.1016/B978-0-12-394316-3.00006-5 [PubMed: 23177987]

Piermarini PM, Akuma DC, Crow JC, Jamil TL, Kerkhoff WG, Viel KCMF, Gillen CM, 2017. Differential expression of putative sodium-dependent cation-chloride cotransporters in Aedes aegypti. Comp. Biochem. Physiol. A. Mol. Integr. Physiol 214, 40–49. 10.1016/j.cbpa.2017.09.007 [PubMed: 28923771]

Ponce-Coria J, San-Cristobal P, Kahle KT, Vazquez N, Pacheco-Alvarez D, de los Heros P, Juárez P, Muñoz E, Michel G, Bobadilla NA, Gimenez I, Lifton RP, Hebert SC, Gamba G, 2008. Regulation of NKCC2 by a chloride-sensing mechanism involving the WNK3 and SPAK kinases. Proc. Natl. Acad. Sci 105, 8458–8463. 10.1073/pnas.0802966105 [PubMed: 18550832]

Rodan AR, 2024. Circadian Rhythm Regulation by Pacemaker Neuron Chloride Oscillation in Flies. Physiology 39, 157–166. 10.1152/physiol.00006.2024

Rodan AR, 2018. WNK-SPAK/OSR1 signaling: lessons learned from an insect renal epithelium. Am. J. Physiol.-Ren. Physiol 315, F903–F907. 10.1152/ajprenal.00176.2018

Rodan AR, Baum M, Huang C-L, 2012. The *Drosophila* NKCC Ncc69 is required for normal renal tubule function. Am. J. Physiol. - Cell Physiol 303, C883–C894. 10.1152/ajpcell.00201.2012 [PubMed: 22914641]

Sawyer DB, Beyenbach KW, 1985. Dibutyryl-cAMP increases basolateral sodium conductance of mosquito Malpighian tubules. Am. J. Physiol 248, R339–45. [PubMed: 2579589]

Schellinger JN, Sun Q, Pleinis JM, An S-W, Hu J, Mercenne G, Titos I, Huang C-L, Rothenfluh A, Rodan AR, 2022. Chloride oscillation in pacemaker neurons regulates circadian rhythms through a chloride-sensing WNK kinase signaling cascade. Curr. Biol 32, 1429–1438.e6. 10.1016/j.cub.2022.03.017 [PubMed: 35303418]

Sobczak K, Bangel-Ruland N, Leier G, Weber W, 2010. Endogenous transport systems in the Xenopus laevis oocyte plasma membrane. METHODS 51, 183–189. 10.1016/j.ymeth.2009.12.001 [PubMed: 19963061]

Wu Y, Schellinger JN, Huang C-L, Rodan AR, 2014. Hypotonicity Stimulates Potassium Flux through the WNK-SPAK/OSR1 Kinase Cascade and the Ncc69 Sodium-Potassium-2-Chloride Cotransporter in the *Drosophila* Renal Tubule. J. Biol. Chem 289, 26131–26142. 10.1074/jbc.M114.577767 [PubMed: 25086033]

Yang X, Wang Q, Cao E, 2020. Structure of the human cation–chloride cotransporter NKCC1 determined by single-particle electron cryo-microscopy. Nat. Commun 11, 1016. 10.1038/s41467-020-14790-3

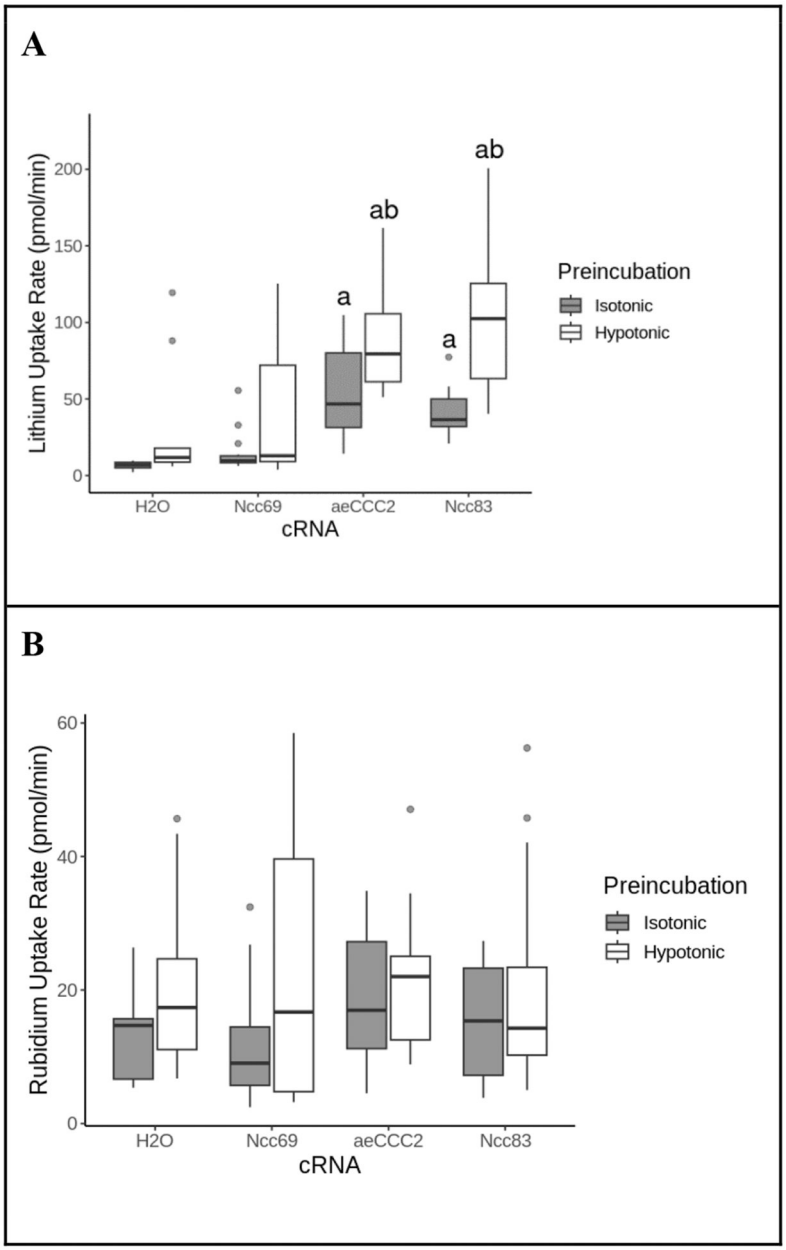

Figure 1.

Effect of hypotonic preincubation on Li^+ and Rb^+ uptake. Lithium (A) and rubidium (B) uptake rates of *Xenopus* oocytes injected with cRNA or H2O control during incubation in a 20mM Li^+/ 5mM Rb^+ flux solution following a 15 minute preincubation in hypotonic ND96/2 or isotonic ND96. Outliers are represented by gray circles, treatments labeled "a" are statistically different from the H2O control group; treatments labeled "b" are statistically different from the isotonic control group within the same cRNA. Li^+ uptake rates were greater in both aeCCC2 and Ncc83-injected oocytes following hypotonic incubation compared to isotonic incubation (ANOVA, $F_{cRNA}=25$, $p_{cRNA}<<0.01$, $F_{Preincubation}=44$, $p_{Preincubation}<<0.01$, n = 8–21 per treatment). Rb^+ uptake was greater following hypotonic

pre-incubation but not affected by cRNA injection (ANOVA, $F_{cRNA}=0.56$, $p_{cRNA}=0.64$, $F_{Preincubation}=6.8$, $p_{Preincubation}=0.010$, n = 8–21 per treatment).

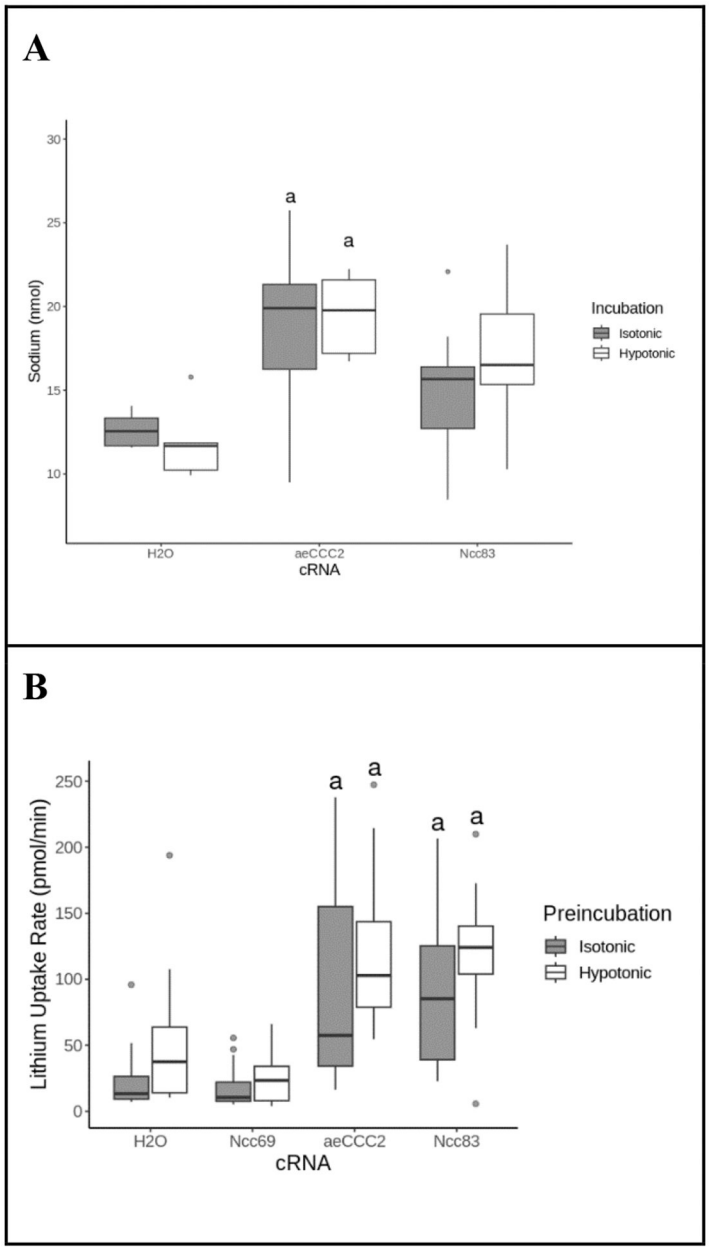

Figure 2.

Effect of ouabain. (A) Internal Na^+ concentration of *Xenopus* oocytes injected with aeCCC2, Ncc83, or H2O after exposure to 1 mM ouabain and incubation in isotonic ND96 or hypotonic ND96/2 for 55 minutes. Outliers are represented by gray circles, treatments labeled "a" are statistically different from the H2O control group. Na^+ concentration is higher in oocytes injected with Ncc83 and aeCCC2 after exposure to ouabain (ANOVA, $F_{cRNA} = 12$, $P_{cRNA} << 0.01$, $F_{Incubation} = 1.82$, $p_{Incubation} = 0.18$ n = 5–15 per treatment). (B) Lithium uptake of *Xenopus* oocytes injected with cRNA or H2O control after exposure to ouabain and incubation in a 20mM Li^+ flux solution. Outliers are represented by gray circles, treatments labeled "a" are statistically different from the H2O control group. Ncc83 and aeCCC2-injected oocytes maintain a higher Li^+ uptake rate in comparison to H_2O

controls during exposure to ouabain (ANOVA, F_{cRNA}= 51, p_{cRNA}<<0.01, $F_{Preincubaiton}$=17, $p_{Preincubation}$<<0.01, n =11–24 per treatment).

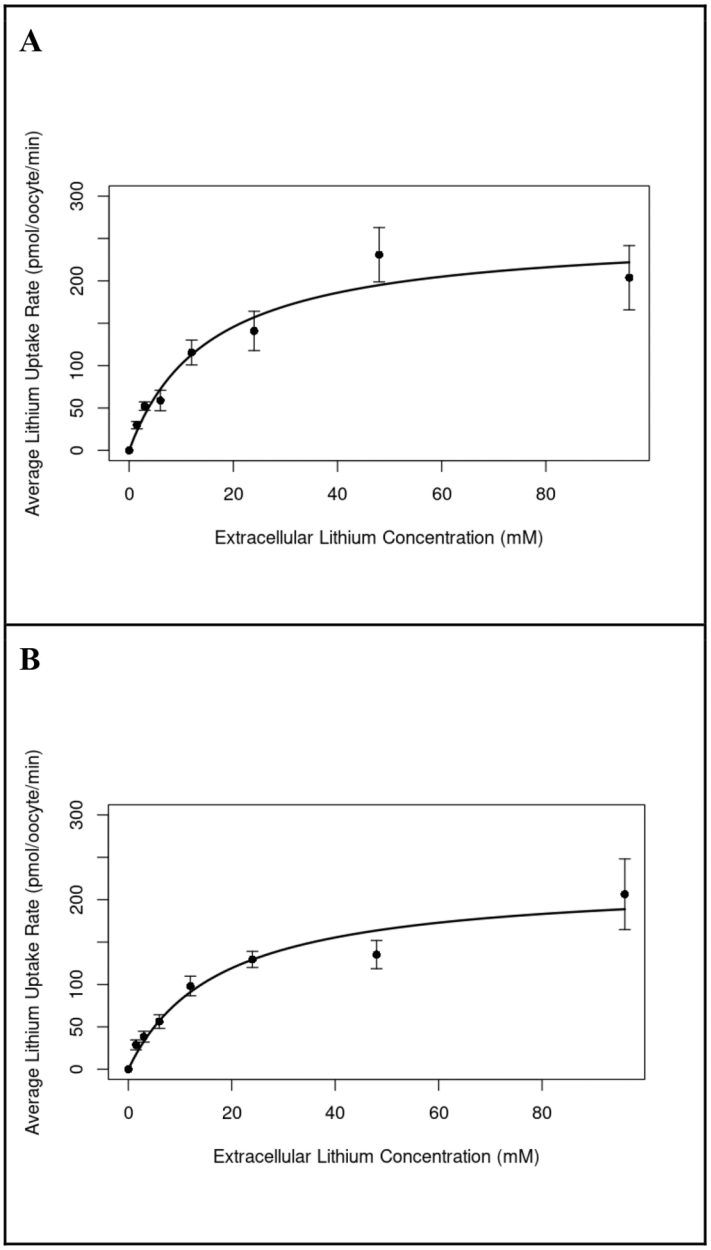

Figure 3.

Lithium uptake with increasing extracellular [Li^+]. Representative curves summarizing four separate experiments measuring Li^+ uptake rate of *Xenopus* oocytes injected with aeCCC2 (A) and Ncc83 (B) in response to incubation in a range of extracellular Li^+ concentrations. The best fit curves are derived from the Michaelis-Menten kinetics equation. Both curves are averages of all Li^+ curve trials, but two Ncc83 trials with linear concentration curves were removed from analysis. Li^+ uptake rate saturates in both Ncc83 (K_m-Ncc83 = 10.61, n=9–12 per treatment) and aeCCC2 (K_m= 20.10, n=11–12 per treatment) as extracellular Li^+ concentration increases.

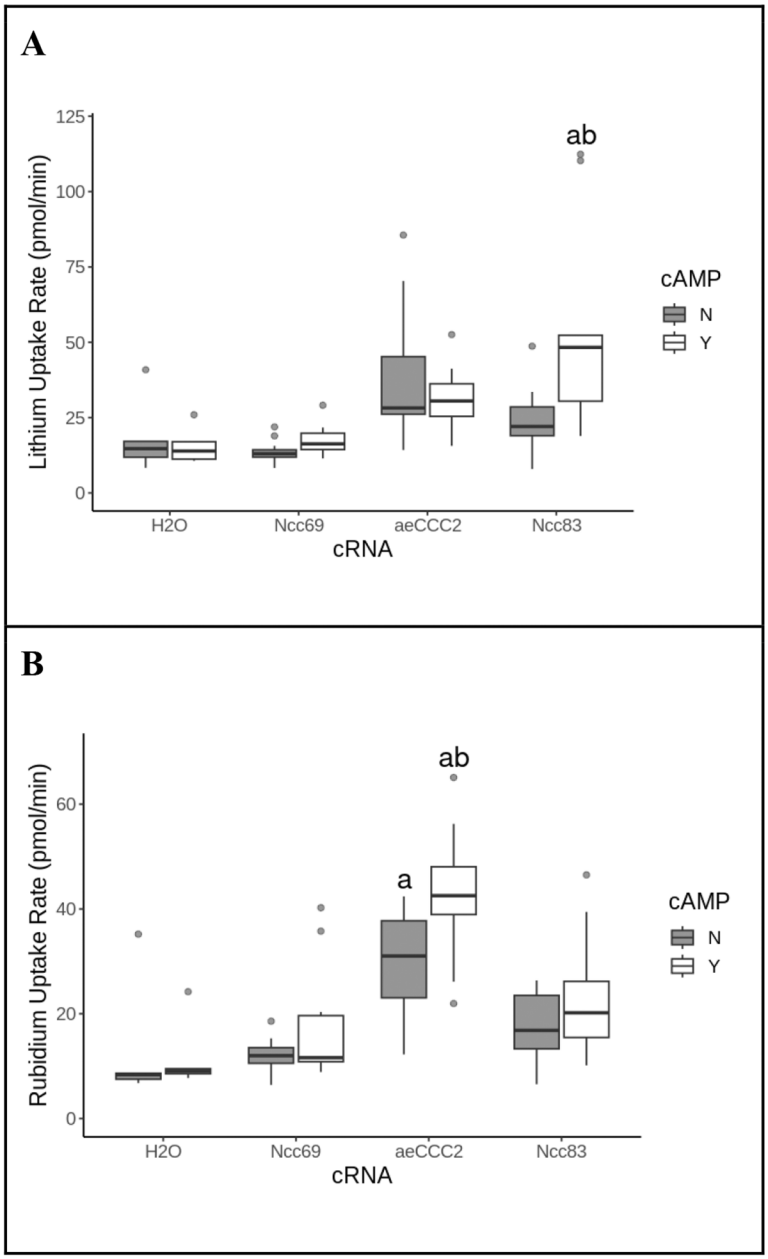

Figure 4.

The effect of cAMP on Li^+ and Rb^+ uptake rate. Li^+ uptake rate (A) and Rb^+ uptake rate (B) of *Xenopus* oocytes injected with cRNA or H2O after exposure to cAMP, isotonic preincubation, and incubation in a 20mM Li^+/ 5mM Rb^+ flux solution. Shaded boxes are no cAMP controls; open boxes are exposure to 1 mM 8-bromo-cAMP. Outliers are represented by gray circles, treatments labeled "a" are statistically different from the H2O control group, and treatments labeled "b" are statistically different from the no cAMP control group within the same cRNA. Exposure to cAMP resulted in an increase in Li^+ uptake for only Ncc83-injected oocytes (ANOVA, F_{cRNA}=13, p_{cRNA}<<0.01, F_{cAMP}=3.3. p_{cAMP}=0.07, n=5–17 per treatment), and an increase in Rb^+ uptake for only aeCCC2-injected oocytes (ANOVA, F_{cRNA}= 57, p_{cRNA}<<0.01, F_{cAMP}=20. p_{cAMP}<<0.01, n=5–17 per treatment).

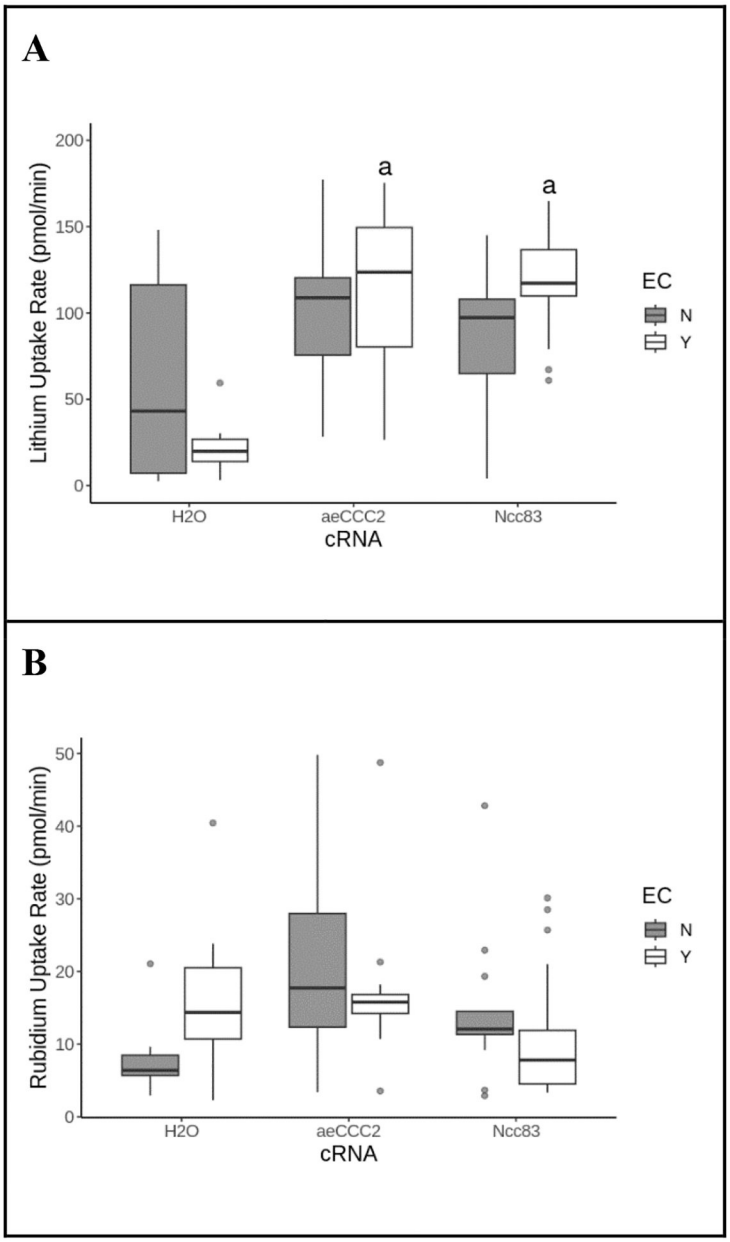

Figure 5.

Ethyl cinnamate (EC) effect Li^+ and Rb^+ uptake rate. Li^+ uptake rate (A) and Rb^+ uptake rate (B) of *Xenopus* oocytes injected with cRNA or H_2O after exposure to ethyl cinnamate (EC), hypotonic preincubation, and incubation in a 20mM Li^+/ 5mM Rb^+ flux solution. Shaded boxes are controls; open boxes are exposure to 5.7 mM EC. Outliers are represented by gray circles, treatments labeled "a" are statistically different from the H2O control group, and treatments labeled "b" are statistically different from the control group within the same cRNA. Exposure to ethyl cinnamate did not abolish the increased Li^+ uptake in Ncc83 and aeCCC2-injected oocytes (ANOVA, F_{cRNA}=17, p_{cRNA}<<0.01, F_{EC}=1.46, p_{EC}=0.23, n = 7–17 per treatment), and exposure to EC had no significant effect on Rb^+ uptake rate (ANOVA, F_{cRNA}=3.7, p_{cRNA}=0.03, F_{EC}=0.42, p_{EC}=0.52, n = 7–17 per treatment).

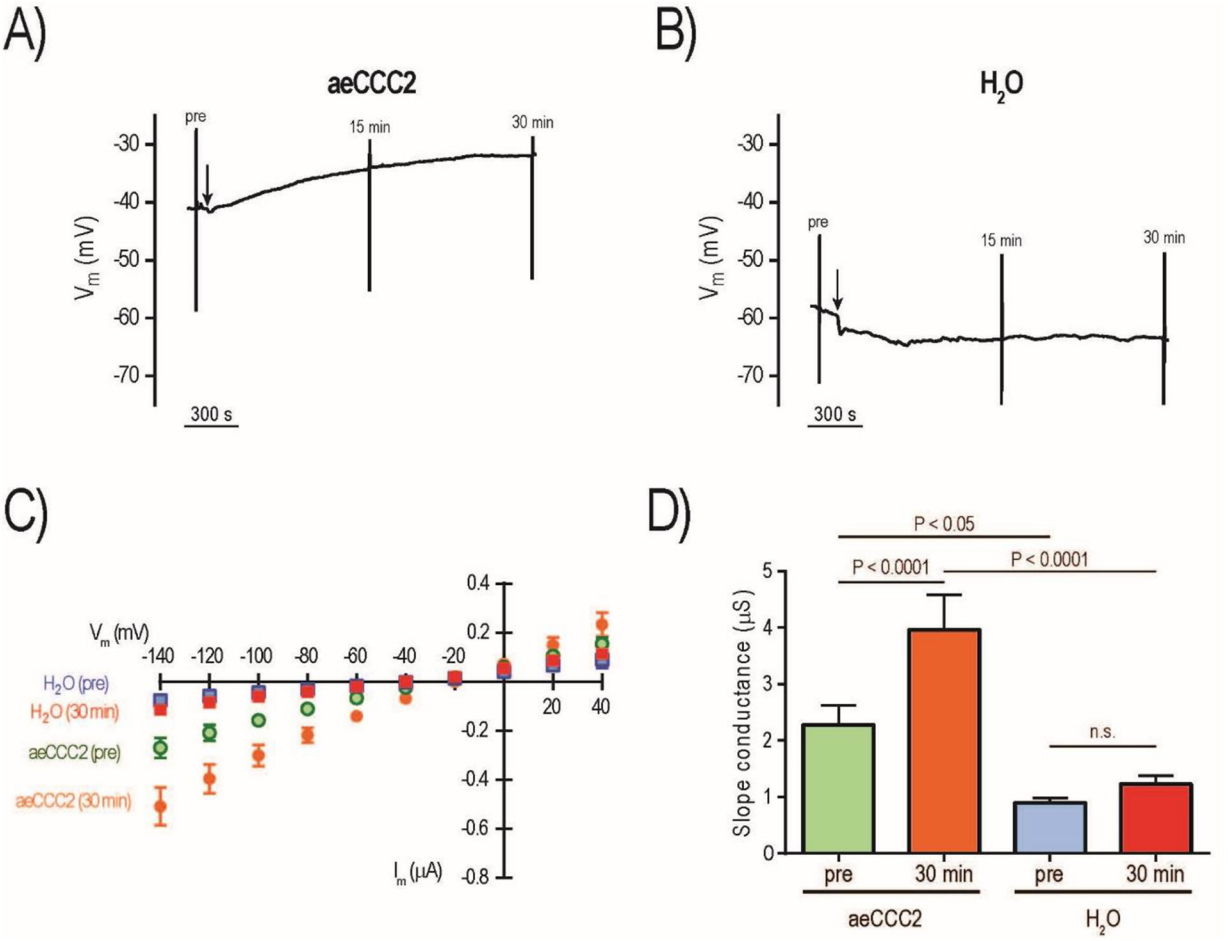

Figure 6:

Effects of 8-Br-cAMP on electrophysiology of aeCCC2 and control (H_2O) oocytes. Representative tracing of V_m in aeCCC2 (A) and H_2O (B) oocytes; vertical lines indicate rapid voltage changes during I-V plot recording before (pre) and after (15 min, 30 min) addition of 1 mM 8-Br-cAMP (arrow). Mean I-V plots of aeCCC2 (circles) and H_2O oocytes (squares) before (pre) and 30 min after addition of 1 mM 8-Br-cAMP (C); values are mean ± SEM (n = 7 oocytes for both aeCCC2 and H_2O). Slope conductances of aeCCC2 and H_2O oocytes before (pre) and 30 min after addition of 1 mM 8-Br-cAMP (D); values are mean ± SEM (n = 7 oocytes for both aeCCC2 and H_2O). P values are from Sidak's multiple comparisons following a repeated measures 2-way ANOVA.

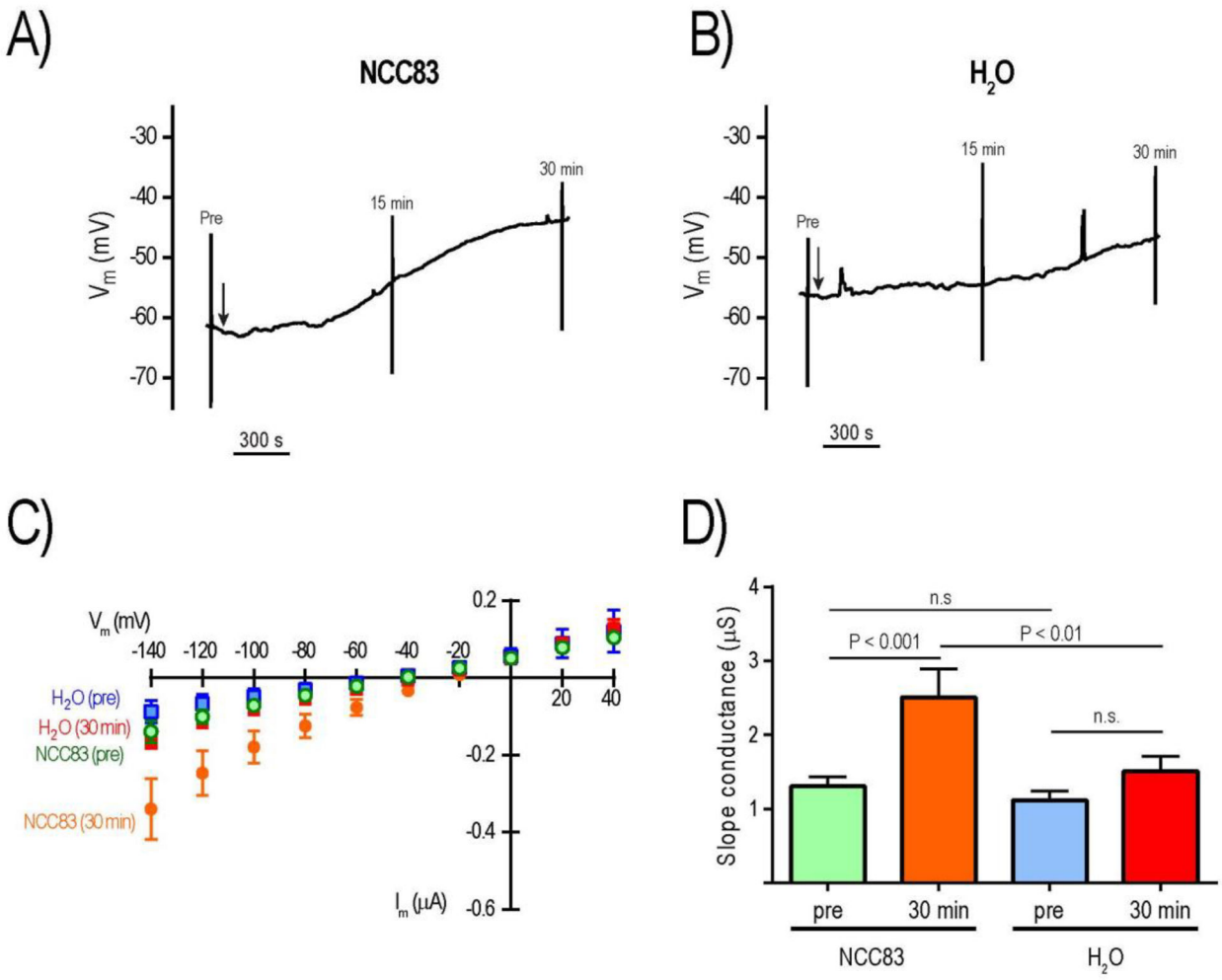

Figure 7:

Effects of 8-Br-cAMP on electrophysiology of Ncc83 and control (H_2O) oocytes. Representative tracing of V_m in Ncc83 (A) and H_2O (B) oocytes; vertical lines indicate rapid voltage changes during I-V plot recording before (pre) and after (15 min, 30 min) addition of 1 mM 8-Br-cAMP (arrow). Mean I-V plots of Ncc83 and H_2O oocytes before (pre) and 30 min after addition of 1 mM 8-Br-cAMP (C); values are mean ± SEM (n = 6 oocytes for Ncc83, n = 8 oocytes for H_2O). Slope conductances of Ncc83 and H_2O oocytes before (pre) and 30 min after addition of 1 mM 8-Br-cAMP (D); values are mean ± SEM (n = 6 oocytes for Ncc83, n = 8 oocytes for H_2O). P values are from Sidak's multiple comparisons following a repeated measures 2-way ANOVA.

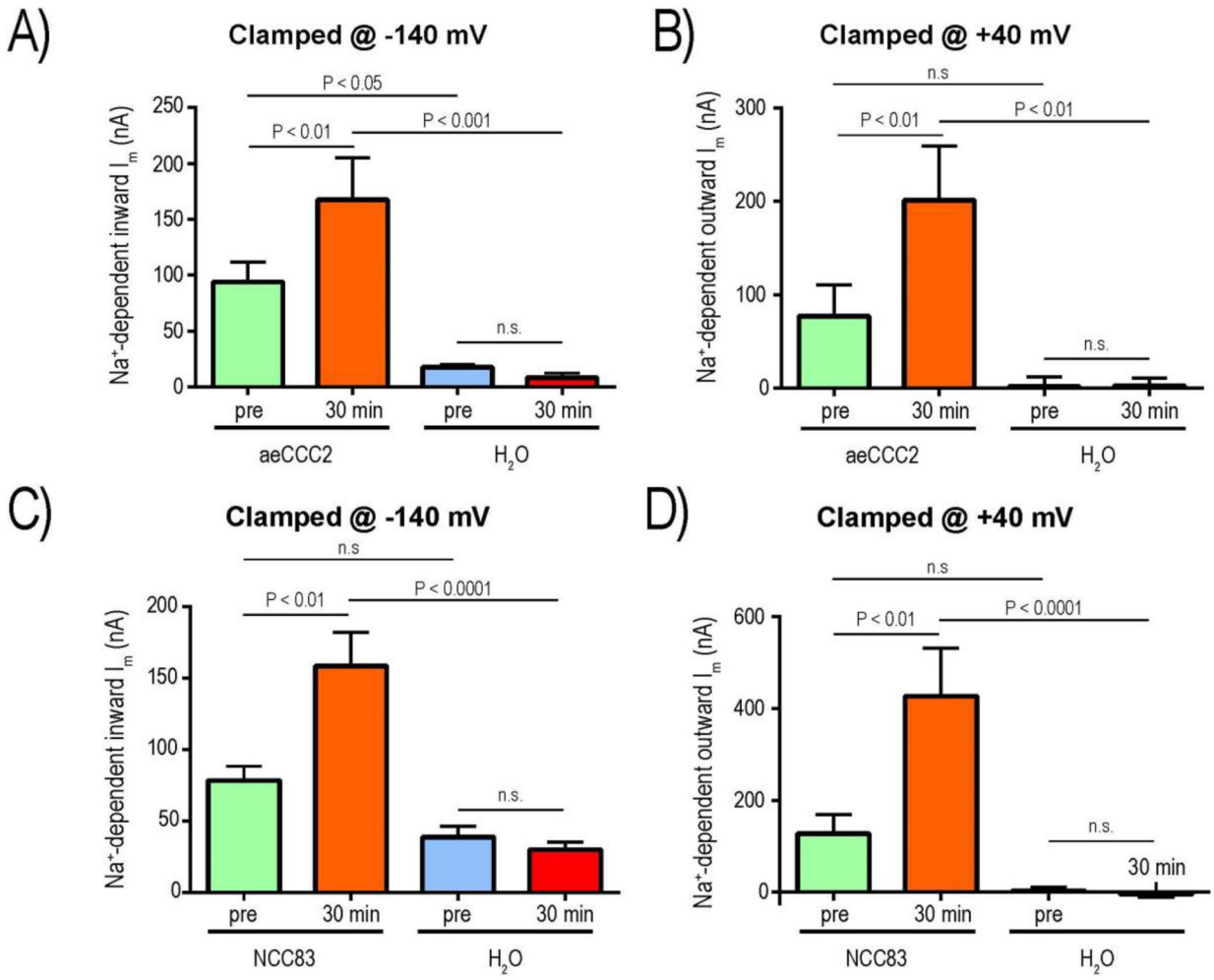

Figure 8:

Effects of 8-Br-cAMP on Na^+-dependent currents of aeCCC2 (A&B) and Ncc83 (C&D) compared to control (H_2O) oocytes. Panels A and C are Na^+-dependent inward currents when oocytes were clamped at −140 mV; panels B and D are Na^+-dependent outward currents when oocytes were clamped at +40 mV. Values are mean ± SEM (n = 5 oocytes for both aeCCC2 and H_2O in A&B; n = 4 oocytes for Ncc83 and n = 5 oocytes for H_2O in C&D). P values are from Sidak's multiple comparisons following a repeated measures 2-way ANOVA.

Table 1:

Cation content of oocytes following flux assay

		Li^+	Na^+	K^+	Mg^{2+}	Ca^{2+}
Isotonic	Water	0.56 ± 0.24	12.2 ± 6.1	59.2 ± 19	4.2 ± 2.5	0.70 ± 0.33
	aeCCC2	1.83 ± 1.9	12.9 ± 7.0	49.0 ± 20	6.4 ± 3.2	0.91 ± 0.36
	Ncc83	0.94 ± 0.43	13.1 ± 5.0	60.4 ± 20	4.7 ± 2.2	0.75 ± 0.28
Hypotonic	Water	1.66 ± 2.6	11.6 ± 4.8	49.8 ± 25	5.1 ± 3.4	0.77 ± 0.39
	aeCCC2	3.13 ± 1.8	12.3 ± 7.1	50.2 ± 22	6.7 ± 3.1	1.00 ± 0.58
	Ncc83	2.25 ± 0.95	11.7 ± 5.5	55.6 ± 17	4.5 ± 2.6	0.68 ± 0.28

Values are mean ± sd; nmol/cell; n = 11–18 per treatment.

Table 2:

Anion content of oocytes following flux assay.

		Cl^-	PO_4^{2-}
Isotonic	Water	41 ± 6.1	2.4 ± 0.7
	aeCCC2	38 ± 11	1.6 ± 1.2
	Ncc83	41 ± 7.1	2.9 ± 1.7
Hypotonic	Water	41 ± 6.5	2.8 ± 0.4
	aeCCC2	41 ± 7.4	2.2 ± 1.0
	Ncc83	40 ± 6.7	2.3 ± 1.4

Values are mean ± sd; nmol/cell; n = 11–18 per treatment.